AD-A092 990 ROME AIR DEVELOPMENT CENTER GRIFFISS AFB NY F/G 17/9
ANTENNA TECHNOLOGY FOR SPACE-BASED RADAR, PART 2, ESTIMATION OF--ETC(U)
JUL 80 R L FANTE, H L SOUTHALL
UNCLASSIFIED RADC-TR-79-358-PT-2 NL

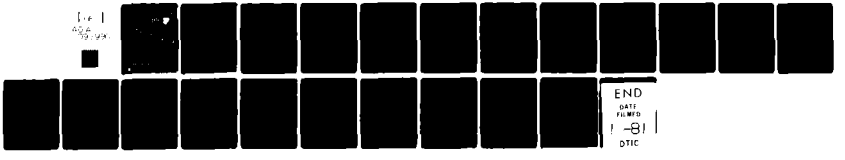

END
DATE FILMED
1-81
DTIC

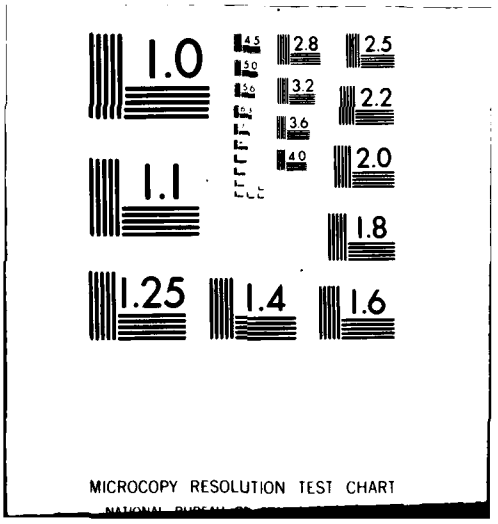
1.0
1.1
1.25
1.4
1.6
1.8
2.0
2.2
2.5
2.8
3.2
3.6
4.0
4.5
5.0
5.6
MICROCOPY RESOLUTION TEST CHART

RADC-TR-79-358
In-House Report
July 1980

LEVEL III

ANTENNA TECHNOLOGY FOR SPACE-BASED RADAR
PART 2. ESTIMATION OF BLOCKAGE SIDE-LOBE LEVELS FOR THE SPACE-BASED RADAR ANTENNA

Ronald L. Fante
Hugh L. Southall, Capt, USAF

ROME AIR DEVELOPMENT CENTER
Air Force Systems Command
Griffiss Air Force Base, New York 13441

This report has been reviewed by the RADC Public Affairs Office (PA) and is releasable to the National Technical Information Service (NTIS). At NTIS it will be releasable to the general public, including foreign nations.

RADC-TR-79-358 has been reviewed and is approved for publication.

APPROVED: Walter Rotman

WALTER ROTMAN, Chief
Antennas & RF Components Branch
Electromagnetic Sciences Division

APPROVED: Allan C. Schell

ALLAN C. SCHELL, Chief
Electromagnetic Sciences Division

FOR THE COMMANDER: John P. Huss

JOHN P. HUSS
Acting Chief, Plans Office

SUBJECT TO EXPORT CONTROL LAWS

This document contains information for manufacturing or using munitions of war. Export of the information contained herein, or release to foreign nationals within the United States, without first obtaining an export license, is a violation of the International Traffic in Arms Regulations. Such violation is subject to a penalty of up to 2 years imprisonment and a fine of $100,000 under 22 U.S.C 2778.

Include this notice with any reproduced portion of this document.

If your address has changed or if you wish to be removed from the RADC mailing list, or if the addressee is no longer employed by your organization, please notify RADC (EEA) Hanscom AFB MA 01731. This will assist us in maintaining a current mailing list.

Do not return this copy. Retain or destroy.

Unclassified

SECURITY CLASSIFICATION OF THIS PAGE (When Data Entered)

REPORT DOCUMENTATION PAGE	READ INSTRUCTIONS BEFORE COMPLETING FORM
1. REPORT NUMBER: RADC-TR-79-358 Pt 2	2. GOVT ACCESSION NO.: AD-A092 990
3. RECIPIENT'S CATALOG NUMBER:	
4. TITLE (and Subtitle): ANTENNA TECHNOLOGY FOR SPACE-BASED RADAR. Part 2. Estimation of Blockage Side-Lobe Levels for the Space-Based Radar Antenna.	5. TYPE OF REPORT & PERIOD COVERED: Final, In-House.
	6. PERFORMING ORG. REPORT NUMBER:
7. AUTHOR(s): Ronald L. Fante; Hugh L. Southall, Capt, USAF	8. CONTRACT OR GRANT NUMBER(s):
9. PERFORMING ORGANIZATION NAME AND ADDRESS: Deputy for Electronic Technology (RADC/EEA) Hanscom AFB Massachusetts 01731	10. PROGRAM ELEMENT, PROJECT, TASK AREA & WORK UNIT NUMBERS: 62702F 46001401
11. CONTROLLING OFFICE NAME AND ADDRESS: Deputy for Electronic Technology (RADC/EEA) Hanscom AFB Massachusetts 01731	12. REPORT DATE: July 1980 13. NUMBER OF PAGES: 19
14. MONITORING AGENCY NAME & ADDRESS (if different from Controlling Office)	15. SECURITY CLASS. (of this report): Unclassified 15a. DECLASSIFICATION DOWNGRADING SCHEDULE

16. DISTRIBUTION STATEMENT (of this Report)

Approved for public release; distribution unlimited.

17. DISTRIBUTION STATEMENT (of the abstract entered in Block 20, if different from Report)

18. SUPPLEMENTARY NOTES

19. KEY WORDS (Continue on reverse side if necessary and identify by block number)

Phased array antenna
Microwave lens
Sidelobes
Radar
Antennas
Radiation patterns

20. ABSTRACT (Continue on reverse side if necessary and identify by block number)

Side-lobe levels due to blockage effect of the boom connecting the feed to the lens of the space-based radar antenna are estimated. Also, the effect of antenna stays on side-lobe levels is calculated. It is shown that side-lobe levels exceeding -50 dB are produced by the boom.

DD FORM 1 JAN 73 1473 EDITION OF 1 NOV 65 IS OBSOLETE

Unclassified

SECURITY CLASSIFICATION OF THIS PAGE (When Data Entered)

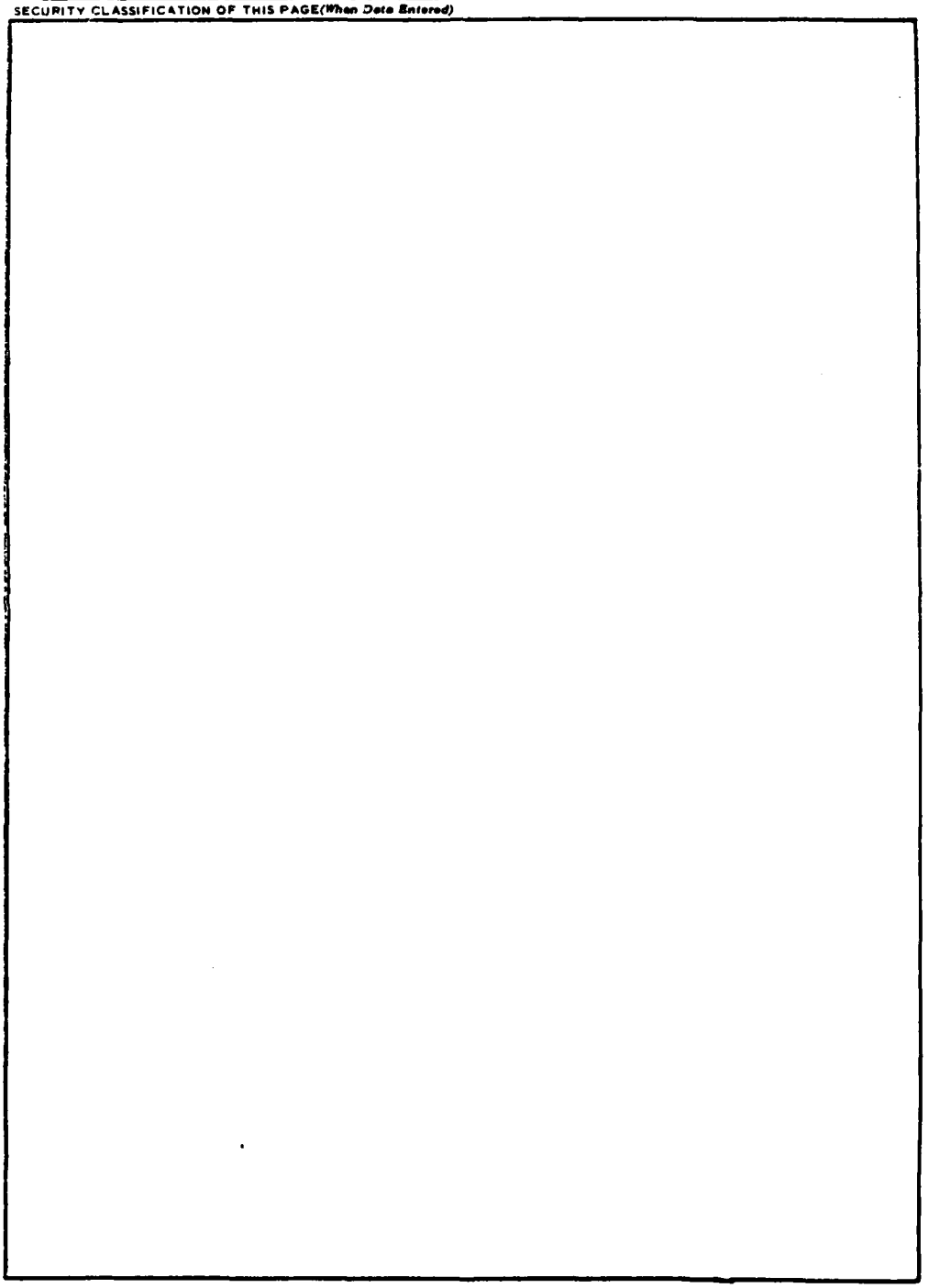

Contents

Illustrations

Illustrations

Antenna Technology for Space-Based Radar

Part 2. Estimation of Blockage Side-Lobe Levels for the Space-Based Radar Antenna

1. *INTRODUCTION*

A large space-fed lens antenna has been proposed for the low side-lobe, deep, steerable null requirements of the space-based radar system. One of the concepts for positioning the antenna feed subsystem relative to the array lens is shown in Figure 1, where a mast structure connects the feed array and the large array lens. For this concept, it appears that scattering caused by the aperture blockage of the triangular mast support members can increase the side-lobe levels of the far-field radiation pattern above the specified -50 dB level.

This report presents estimates of side-lobe levels produced by this blockage effect. First, side-lobe levels are estimated using an approximate expression for the field between the feed and the array aperture (lens). Then a more exact expression for this field is used in order to obtain more accurate estimates of blockage side-lobe levels. This more exact field expression includes the effect of the subarray beams in the space-feed concept. Detailed side-lobe structure is presented for the case where the more exact field representation is used. In addition, blockage side-lobe levels for antenna stays are estimated.

(Received for publication 21 July 1980)

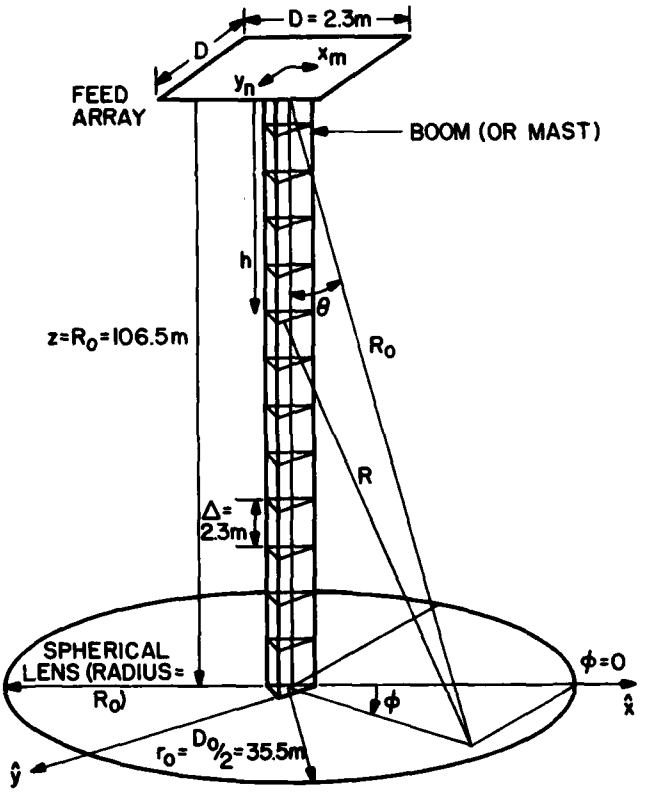

Figure 1. Geometry and Dimensions for the Space-Based Radar Antenna

2. SIDE LOBES DUE TO SCATTERING BY ELEMENTS ON THE SUPPORT BOOM (APPROXIMATE FIELD)

First, consider the system side lobes produced by scattering from the boom. The vertical boom structure is relatively unimportant, since the vertical field component is small when compared with the horizontal.

Let us *therefore ignore vertical and near vertical support elements on the* boom so that scattering is mainly by the horizontal, triangular elements shown in Figure 1. There are 51 triangular support members, each with three equal sides assumed to be circular bars 0.44 m long, with a radius of 0.00574 m. We also use reciprocity, so that side lobes on receive can be analyzed by considering the radiation pattern on transmit. A first approximation for the field along the mast is given by

$$\underline{E}(h) = \frac{\hat{x}\, E_o\, e^{-jkh}}{\left[1 + \frac{h^2\lambda^2}{4D^4}\right]^{1/2}} \tag{1}$$

where $k = 2\pi/\lambda$, D is the feed aperture dimension, $\hat{x}$ a unit vector and h distance measured from the feed array toward the lens. Note that Eq. (1) represents a collimated beam for $h < 2D^2/\lambda$ and a spherical wave for $h \gg 2D^2/\lambda$. The field is linearly polarized in the $\hat{x}$ direction. In the next section, we will consider an improved representation for $\underline{E}(h)$. Figure 2 shows an expanded picture of one of the horizontal triangular supports.

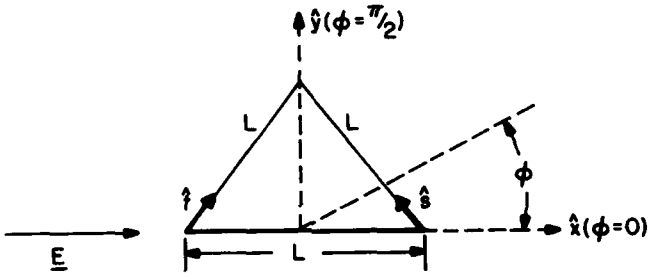

Figure 2. Detailed View of Triangular Support Member
(view from lens toward feed array)

When the field is incident on one of the legs of the triangular sections shown in Figure 2, the current induced in that leg is given by

$$I = \frac{4\omega\epsilon_o\, \underline{E}(h) \cdot \hat{l}}{k^2\, H_o^{(2)}(ka)} \tag{2}$$

where

$\hat{l}$ = a unit vector along the triangle leg

ω = radian frequency

ϵ_o = permittivity of vacuum

$H_o^{(2)}$ = the Hankel function of the second kind

a = the radius of the element.

For $a \ll \lambda$, Eq. (2) can be approximated by

$$I \simeq \frac{j 2\pi \underline{E}(h) \cdot \hat{l}}{\omega \mu_o \left[\ln\left(\frac{5.6a}{\lambda}\right) + j\frac{\pi}{2} \right]} \tag{3}$$

where μ_o is the permeability of vacuum and $\omega = 2\pi f$. Note that $\hat{l}$ is one of the unit vectors $\hat{t}$, $\hat{s}$ or $\hat{x}$ in Figure 2.

The current produces a vector potential near the lens given by

$$\underline{A} = \frac{\hat{l}}{4\pi} \int dl\, I\, \frac{e^{-jkR}}{R} \tag{4}$$

where R is the distance from a point on the scattering element to a field point. The magnetic field $\underline{H}$ is calculated from Eq. (4) via $\underline{H} = \nabla \times \underline{A}$. For a triangle located a distance h from the feed, the vector potential at a point x, y, z is given by

$$\begin{aligned} \underline{A} = {} & \frac{jL\underline{E}(h)}{4\pi\mu_o f \left[\ln\left(\frac{5.6a}{\lambda}\right) + j\frac{\pi}{2} \right]} \left(\frac{e^{-jkr}}{r}\right) \left\{ \hat{x}\, \mathrm{sinc}\left[\frac{kLx}{2r}\right] \right. \\ & + 0.5(0.5\hat{x} - 0.866\hat{y}) \exp\left\{ j\frac{kL}{r}\left(\frac{x}{4} + 0.433y\right)\right\} \mathrm{sinc}\left\{\frac{kL}{2}\left(0.5\frac{x}{r} - 0.866\frac{y}{r}\right)\right\} \\ & \left. + 0.5(0.5\hat{x} + 0.866\hat{y}) \exp\left\{ j\frac{kL}{r}\left(-\frac{x}{4} + 0.433y\right)\right\} \mathrm{sinc}\left\{\frac{kL}{2}\left(0.5\frac{x}{r} + 0.866\frac{y}{r}\right)\right\} \right], \end{aligned} \tag{5}$$

where

$$r = [x^2 + y^2 + (z - h)^2]^{1/2}$$

and

$$\mathrm{sinc}\ \alpha \equiv \frac{\sin \alpha}{\alpha} .$$

In Eq. (4), and as shown in Figure 1, R is taken to be the distance from a point on a scattering element (triangular support member) to a field point. However, in Eq. (5), R is approximated by r, the distance from the center of a

triangular support member to a field point x, y, z. The total vector potential is obtained by summing the vector potentials due to each triangle. This ignores any mutual coupling between triangles. Let

$$h = n\Delta$$

and for each triangle

$$R \approx r_n \quad ,$$

where

$$r_n = R_o \left[1 + \left(\frac{n\Delta}{R_o} \right)^2 - 2 \frac{n\Delta}{R_o} \cos \theta \right]^{1/2}$$

is the distance from the center of the nth triangle to a point on the lens located by the lens radius of curvature, R_o, and the angle θ. This analysis is applicable strictly to a spherical lens with a radius $R_o = 106.5$ m. For a flat face lens located a distance z from the feed, R_o would be a function of x and y; that is, $R_o = \sqrt{z^2 + x^2 + y^2}$. *However, near the lens center and for z large, the scattered field will approximate the field scattered upon a flat face lens.*

In Eq. (5) for the vector potential, use $x/r_n = g_n \sin\theta \cos\phi$ and $y/r_n = g_n \sin\theta \sin\phi$, where $g_n = [1 + (n\Delta/R_o)^2 - 2\, n\Delta/R_o \cos\theta]^{-1/2}$ and n is the summation index. Upon summing over all triangles and taking the curl (in order to get the $\underline{H}$ field), we find for the normalized magnetic field

$$H_y = \sum_{n=1}^{51} V_n \left\{ \text{sinc}\,(\alpha g_n) + \frac{1}{4} e^{jbg_n} \text{sinc}\,(ag_n) + \frac{1}{4} e^{jag_n} \text{sinc}\,(bg_n) \right\} \qquad (6)$$

$$H_x = -0.433 \sum_{n=1}^{51} V_n \left\{ -e^{jbg_n} \text{sinc}\,(ag_n) + e^{jag_n} \text{sinc}\,(bg_n) \right\} \qquad (7)$$

where

$$V_n = \frac{A_o e^{-jkn\Delta}}{\sqrt{1 + \left(\frac{n\lambda\Delta}{2D^2}\right)^2}} \left(\frac{R_o \cos\theta - n\Delta}{r_n}\right) \frac{e^{-jkr_n}}{r_n} \tag{8}$$

and

$$A_o = \frac{L}{2} \frac{\left[1 + \left(\frac{R_o\lambda}{2D^2}\right)^2\right]^{1/2}}{\left[\ln\left(\frac{5.6a}{\lambda}\right) + j\frac{\pi}{2}\right]} \tag{9}$$

$$r_n = \frac{R_o}{g_n} \tag{10}$$

$$a = -0.5\alpha + 0.866\beta \tag{11}$$

$$b = 0.5\alpha + 0.866\beta \tag{12}$$

$$\alpha = \frac{kL}{2} \sin\theta \cos\phi \tag{13}$$

$$\beta = \frac{kL}{2} \sin\theta \sin\phi \tag{14}$$

In Eqs. (6) and (7) the magnetic field has been normalized to the magnetic field which would be present at the center of the lens in the absence of the support mast, that is, no scattering at all.

The relative power near the lens center scattered by the triangular (horizontal) support elements in the mast is shown in Figure 3 for λ = 25 cm. The relative power near the lens edge is shown in Figure 4. There is no sharp null structure, since the field point is in the near field of some of the scatterers. Note also that the variation along the x-axis (ϕ = 0) is similar to that along the y-axis ($\phi = \pi/2$), especially for small θ.

The scattered power near the lens center is only about -10 dB relative to the unscattered power there; this produces effective blockage side lobes of order

$$SL \simeq 10 \log_{10}\left[0.1\left(\frac{\theta_B}{\theta_1}\right)^4\right] \tag{15}$$

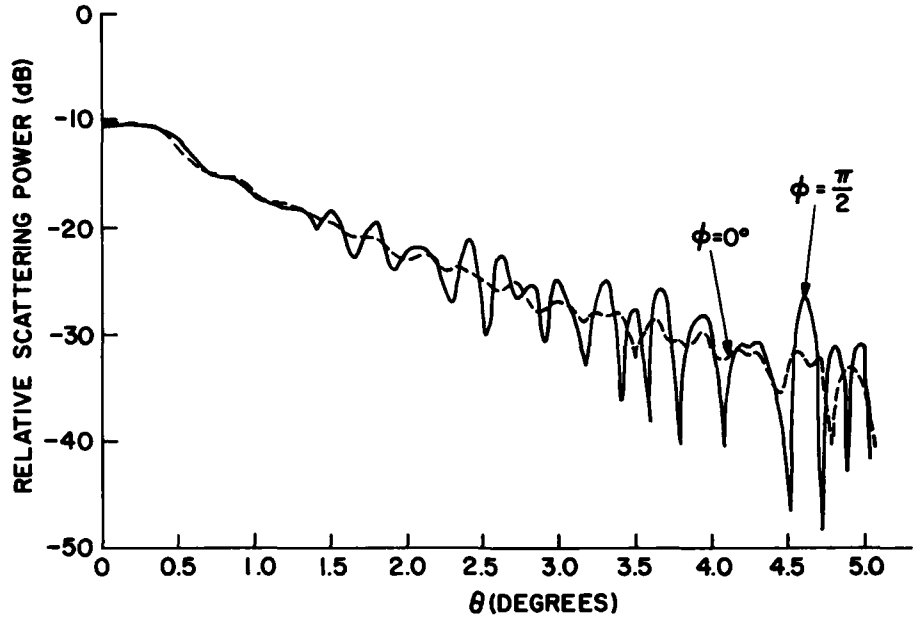

Figure 3. Boom Scattered Power on Lens Relative to Unscattered Power at Center of Lens for Small θ; λ = 25 cm

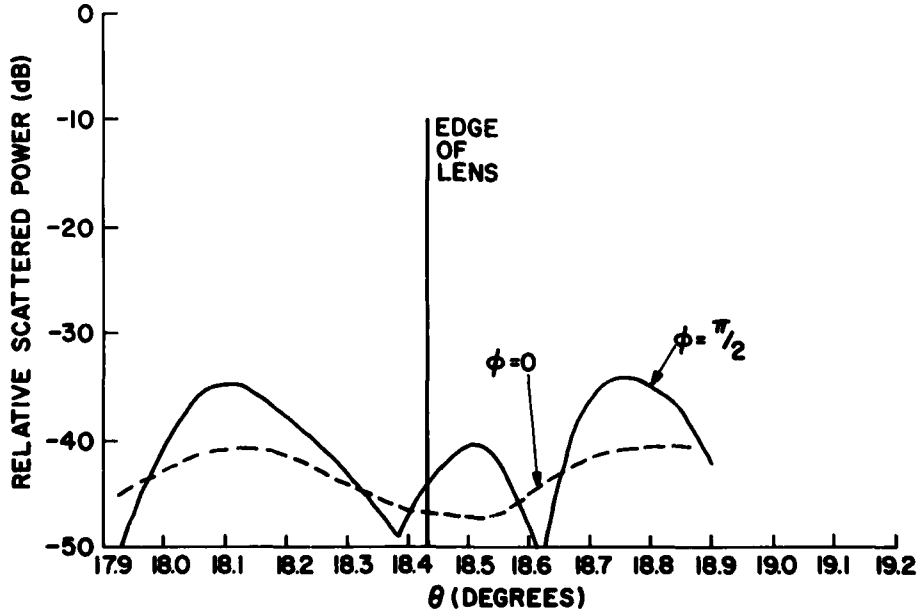

Figure 4. Boom Scattered Power on Lens Relative to Unscattered Power at Center of Lens for Large θ; λ = 25 cm

where θ_B is the beam width of the scattered pattern in Figure 3 and θ_1 the angle subtended by the edge of the lens. From Figure 3 we see that θ_B is of order 0.5° to 0.9°, whereas $\theta_1 = 18.4^\circ$. Consequently, the blockage side lobes are of order -62 to -72 dB.

3. SIDE LOBES DUE TO SCATTERING BY ELEMENTS ON THE SUPPORT BOOM (MORE ACCURATE FIELD)

Using the approximate field of Eq. (1) and Eqs. (6) and (7) for the scattered field on the lens, we estimate side-lobe levels of -72 to -62 dB. Since these levels are well below the specified -50 dB side-lobe operational requirements of the space-based radar antenna, a more accurate field representation is used for $\underline{E}(h)$ to determine if the assumed form of the field between the feed and the lens has a significant impact upon antenna far-field radiation pattern side-lobe levels. Equations (6) and (7) were used again to calculate the scattered field on the lens. However, V_n was modified to include the correct normalization for the new field representation.

The more accurate expression for the field, which includes the effect of the angular distribution of 37 subarray beams, is given by

$$\underline{E}(h) = \hat{x} \sum_{p=1}^{37} \sum_{m=-M+1}^{M} \sum_{n=-N+1}^{N} I_p \times \frac{\exp[-jk\rho_{nm} - jkx_m \sin\theta_p \cos\phi_p - jky_n \sin\theta_p \sin\phi_p]}{\rho_{nm}} \qquad (16)$$

where

$$\rho_{nm} = \sqrt{h^2 + x_m^2 + y_n^2} \quad .$$

Also, $x_m = (m - 1/2)d$ and $y_n = (n - 1/2)d$ are coordinates on the square feed with 2 M elements separated by the distance d in the x direction, and 2 N elements separated by the same distance in the y direction. The number of feed radiating elements is therefore 2 N × 2 M. Also in Eq. (16), $k = 2\pi/\lambda$, and θ_p and ϕ_p locate the center of the p^{th} subarray beam on the array lens as shown in Figure 5; I_p is the subarray amplitude taper for the p^{th} beam. For example, $I_p = e^{-c\theta_p^2}$ for a Gaussian amplitude taper. The constant c is chosen to make the outermost beam

approximately 30 dB smaller in amplitude than the center beam, that is, $I_p = e^{-3.565(\theta_p/18)^2}$ for θ_p in degrees. Also, 2 M = 2 N = 16, d = $\lambda/2$, and λ = 0.25 m.

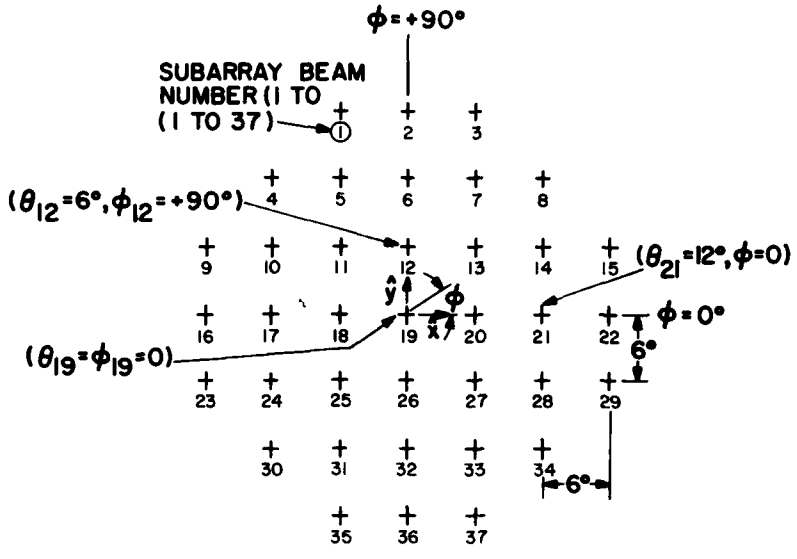

Figure 5. Angular Distribution of the 37 Subarray Beam Centers

The triangular mast supports scatter RF power. The extra "bump" in the illumination on the array lens can be treated as a blockage effect which produces side lobes in the antenna far-field radiation pattern given approximately by

$$SL \approx 10 \log_{10} \left[\frac{P_b}{P_o} \left(\frac{\theta_B}{\theta_1} \right)^4 \right] \tag{17}$$

where P_b/P_o is the ratio of the scattered power at the array center (x = y = 0) to the power which would be present at the center with no scattering; θ_B is the "half beamwidth" of the scattered power distribution and $\theta_1 = 18.4^o$. This assumption is used to compare the previous results with those obtained using the more accurate field representation; in addition, far field patterns are calculated directly from the perturbed aperture illumination in order to determine more detailed information about the side-lobe structure.

The use of Eq. (16) for $\underline{E}(h)$ gives a scattered field distribution designated as $E_{scat.}$ in Figure 6. The distribution was obtained for $\phi = \pi/2$, that is, along the positive y axis; however, the distribution is similar for other values of ϕ, as noted earlier, and is assumed to be circularly symmetric. This lack of ϕ dependence simplifies the calculation of the far-field radiation pattern. The unperturbed field distribution (due to the subarray beams alone, with no scattered field) is designated as E_o in Figure 6, and is also assumed to be circularly symmetric. Both field patterns are normalized to the value of E_o at r = 0, that is, at x = y = 0, which is the lens center.

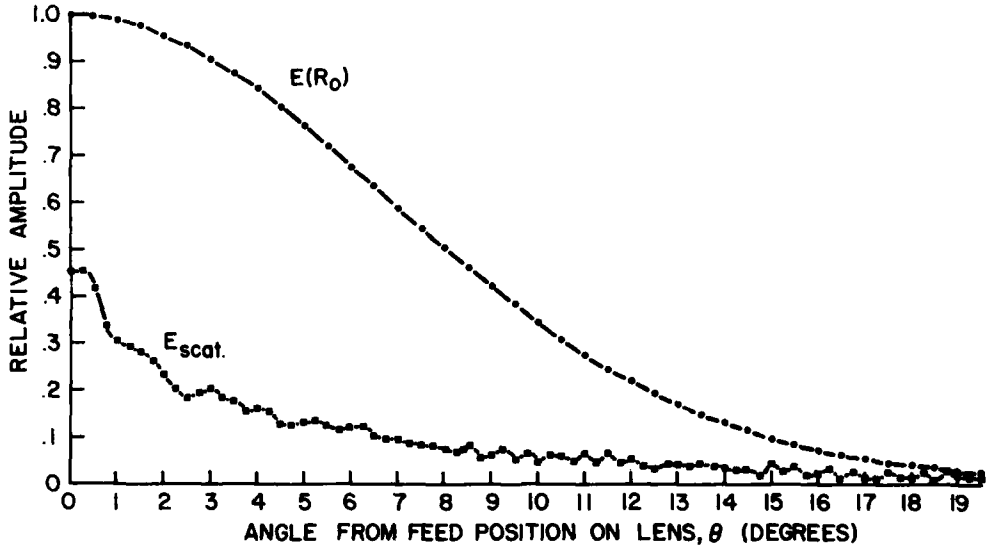

Figure 6. Unperturbed and Scattered Fields on the Lens ($\phi = \pi/2$)

Taking the -3 dB power point as a criterion for the blockage extent, we get $\theta_B \approx 0.8$ degrees (-3 dB in power occurs when the field has decreased to 0.707 of the peak value). Also, $P_b/P_o = (0.46/1.0)^2 = 0.21$; therefore

$$SL \approx 10 \log_{10} \left\{ 0.21 \left[\frac{0.8}{18.4} \right]^4 \right\} \tag{18}$$

$$\approx -61 \text{ dB}$$

Taking the criterion for the extent of blockage as the angle where the field has decreased to half its value at the lens center, we get

$$SL \approx 10 \log_{10} \left\{ 0.21 \left[\frac{2}{18.4} \right]^4 \right\} \tag{19}$$

$$\approx -45 \text{ dB}$$

The side-lobe levels predicted using Eq. (1) for the field range from -72 to -62 dB, depending upon the value used for θ_B in Eq. (17). Therefore, the present analysis predicts higher side-lobe levels.

The results in Eqs. (18) and (19) are approximations for system side-lobe levels.

To obtain more detailed information about side-lobe structure, the field distributions in Figure 6 were used to calculate a far field radiation pattern of the phased array antenna. The far field radiation pattern (for $\theta_o = 0$, scan angle of zero degrees), assuming a circularly symmetric field distribution over a circular aperture of radius r_o (where $r_o = D_o/2$) is given by

$$F(\theta) = \int_0^{r_o} J_o(kr \sin \theta)\, f(r)\, r\, dr \tag{20}$$

where $J_o(kr \sin \theta)$ is the zeroth order Bessel function, f(r) the field distribution on the array aperture and, θ (in this case) the far field angle from array normal (broadside). In the worst case, E_{scat} is either 180^o out of phase with E_o and $f(r) = E_o - E_{scat}$, or exactly in phase where $f(r) = E_o + E_{scat}$. These conditions imply phase coherence between the scattered field and unperturbed field. For conditions where the phase between the scattered and unperturbed field is other than a fixed constant (for example randomly varying), the effect of the scattered field upon the side-lobe structure is expected to be less severe. Curve fits for E_o and E_{scat} were used in Eq. (20), and the integral was numerically evaluated by dividing the radius into 100 equal increments and using the composite Simpson's rule.

Radiation patterns for the case of unperturbed field illumination ($E_{scat} = 0$) and the perturbed cases of 180^o out of phase and in phase are shown in Figures 7, 8, and 9, respectively. Note that, as specified, side lobes are below -50 dB in Figure 7 for $E_{scat} = 0$; however, for both the 180^o out of phase case and the in phase case, the side lobes are above the -50 dB specification and approach -40 dB near the main lobe in Figure 8. In both cases, the side-lobe levels are higher than the $E_{scat} = 0$ condition for far field angles out to four or five degrees.

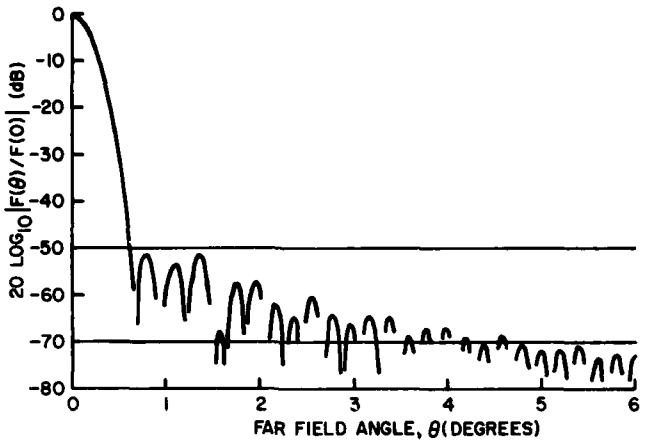

Figure 7. Radiation Pattern for $E_{scat} = 0$

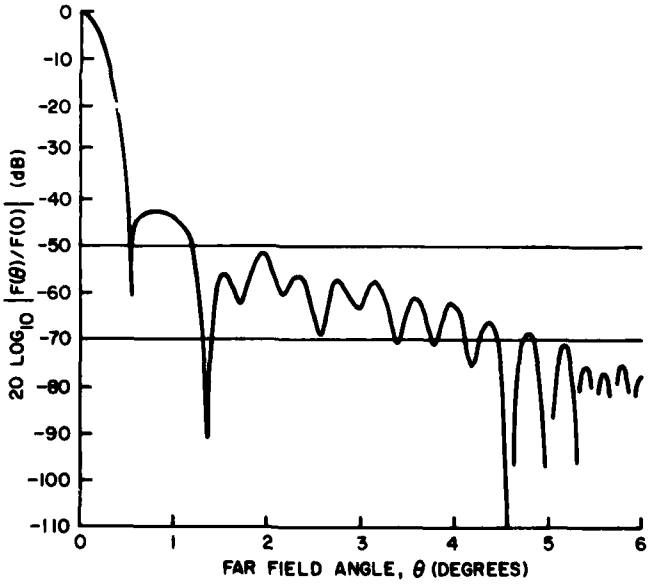

Figure 8. Radiation Pattern for $f(r) = E(R_o) - E_{scat}$ (180^o out of phase case)

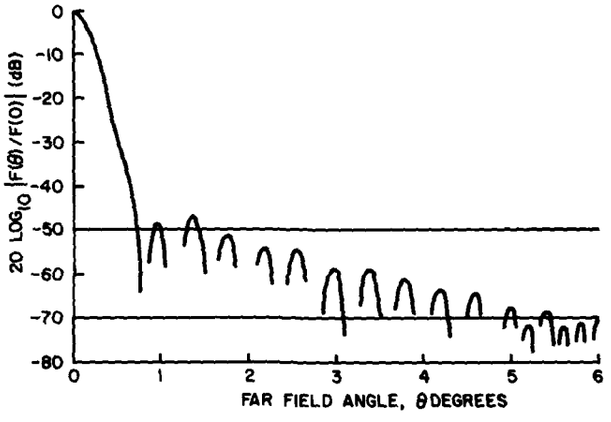

Figure 9. Radiation Pattern for $f(r) = E(R_o) + E_{scat}$ (in phase case)

4. SIDE LOBES DUE TO ANTENNA STAYS

Side lobes due to antenna lens stays can be treated as simple near-field blockage. If the transverse stay width is 2a, its electrical blockage width (assuming $2a \ll \lambda$) is

$$\sigma = \frac{\pi\lambda}{2\left[\ln^2 \frac{5.6a}{\lambda} + \frac{\pi^2}{4}\right]} \tag{21}$$

if the electric field is parallel to the stay. Consequently the electrical blockage area of a single stay-pair is

$$A_b = \sigma D_o \tag{22}$$

where D_o is the lens diameter, as shown in Figure 10.

The blockage side-lobe level produced by a stay-pair oriented parallel to the electric field is shown in Figure 11 for $\lambda = 25$ cm. For $2a = 1''$, $a/\lambda = .05$, we see from Figure 11 that this blockage produces -55 dB sidelobe levels.

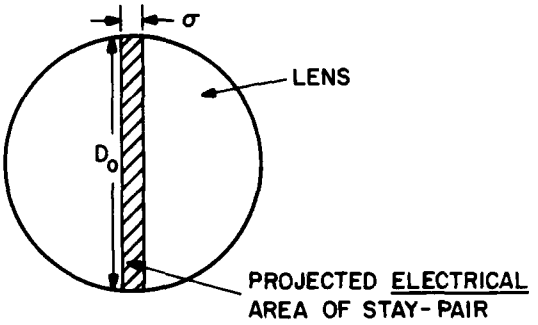

Figure 10. Electrical Blockage Area of a Single Stay-pair

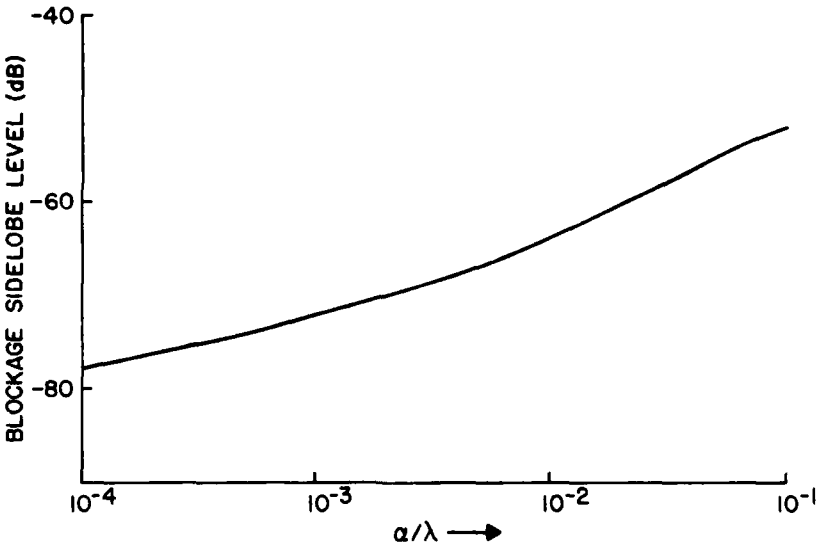

Figure 11. Blockage Side-Lobe Levels Produced by a Pair of Stays Oriented Parallel to E-Field; λ = 25 cm; D_o = 70 m

5. CONCLUSIONS

Side-lobe levels due to the blockage effect of the feed boom and support stays for the space-based radar antenna have been estimated. For the boom, the scattered field from the triangular support members produces far field side lobes in excess of -50 dB and side-lobe levels up to 8 dB higher than the "zero scattering" or unperturbed pattern at angles out to four degrees. In addition, it was shown

that the approximate field representation of Eq. (1) yielded conservative estimates of side-lobe levels compared with the field representation of Eq. (16), in which subarray beams were specifically included. Side-lobe levels due to antenna stays were on the order of -55 dB.

MISSION
of
Rome Air Development Center

RADC plans and executes research, development, test and selected acquisition programs in support of Command, Control Communications and Intelligence (C^3I) activities. Technical and engineering support within areas of technical competence is provided to ESD Program Offices (POs) and other ESD elements. The principal technical mission areas are communications, electromagnetic guidance and control, surveillance of ground and aerospace objects, intelligence data collection and handling, information system technology, ionospheric propagation, solid state sciences, microwave physics and electronic reliability, maintainability and compatibility.